M W Journal of Science

https://doi.org/10.5281/zenodo.10977842 MW Journal of Science, 2024, 1, 1, 8-16

Comparison of Thermal and Electrical Properties of NiNnSn Shape Memory Alloy, and Effects of Thermal Aging on Alloy

Sevim DAĞ[1], Ayşe AYDOĞDU[2], Yıldırım AYDOĞDU[2]*, Ecem ÖZEN ÖNER[3]

[1] Graduate School of Natural and Applied Sciences, Gazi University, Ankara / TÜRKİYE
[2] Department of Physics, Faculty of Science Gazi University, Ankara / TÜRKİYE
[3] Department of Physics, Faculty of Science, Fırat University, Elazig / TÜRKİYE
*Corresponding author: y.aydogdu@gazi.edu.tr

Abstract

The goal of this research is to observe alterations in the structure of the alloy after studying physical parameters such as thermal and electrical properties of the shape memory alloy, which has an atomic percentage of composition of $Ni_{50}Mn_{39}Sn_{11}$. NiMnSn alloy ingots made by arc melting were heat treated at 900 °C for 17 hours in a high purity argon environment, and then alloy cooled in brine-ice water and air. The alloy has been divided into little pieces since it is employed in a variety of physical measurements. DSC measurements on alloy samples were used to estimate phase transformation temperatures, and activation energies were computed based on these data. Electrical measurement results supported the obtained results. Metallographic methods were investigated, and the peak spots from the X-ray diffraction pattern were calculated, allowing the alloy's crystal structure to be determined. This study also looked at the aging effect, which increases the mechanical and functional properties of Ni-based alloy groups.

Keywords: NiMnSn, shape memory alloy, transformation temperatures, activation energy, aging effect

Introduction

Due to the shape memory effect of shape memory alloys, it has provided a wide range of study areas today. In short, it is defined as a material group that can return to its real shape and dimensions. The recovery time determines the size of the shape memory effect of the material. When it comes to shape memory alloys, the first NiTi (Nitinol) alloy group comes to mind [1-3]. Shape memory alloys, which are sensitive to thermal changes, can have two different crystal structures above and below their critical transformation temperatures. Shape memory alloys consist of a kind of sensor that detects the input signal and an actuator that can give an appropriate response to this signal [4-7].

NiTi alloys are more preferred than copper-based and iron-based alloys; elongation, high tensile strength and corrosion resistance. Magnetic shape memory alloys are ferromagnetic materials capable of producing motion and force in mild magnetic fields. MSMAs are typically nickel, manganese, and gallium (Ni-Mn-Ga) alloys. There are other variations to this combination; Sn is used instead of Ga, which is chosen because it decreases prices and shows future promise [8-10]. Ni-Mn-based magnetic shape memory alloys are a family of intermetallic alloy groups that exhibit many different physical properties. Sutou et al. determined magnetic field-induced reverse martensitic transformation and shape memory effect in NiMnX (X = In, Sn, Sb) magnetic shape memory alloys [11, 12]. In similar research, Ni-based shape memory alloys have a significant role in improving functional and mechanical qualities as well as aging. The size

and distribution of Ni precipitates are generally determined by the aging temperature, aging period, external variables, and chemical structure. It is well known in the literature that the size of Ni precipitates grows with increasing aging temperature and time [13-15]. In this study, the aging effect of NiMn-based MSMAs on the detailed microstructural physical properties of the NiMnSn magnetic shape memory alloy was investigated by observing. The cut samples were subjected to certain heat treatments and the regular and irregular phase transitions of the alloys and the temperatures at which these phases occurred were determined [16-18]. The martensite and austenite transformation temperatures, which vary depending on the weight % of the elements in the alloy, were determined by the Differential Scanning Calorimetry (DSC) technique and the shape memory phenomenon was examined. The transformation mechanism of the alloy was determined by electrical resistance-temperature measurements.

The aging process can be defined as a process applied to give strength to the metal by precipitating the alloy material in the structure of the metal. The aim of this study is to increase the strength of the alloy by examining the properties of the alloy based on our previous work [19].

2. Experimental Procedure

NiMnSn shape memory alloys were produced by vacuum arc melting using high purity elements. Since vacuum is applied first in arc melting, the prepared metal powders were turned into pellets in the press machine to prevent the dispersion of metal powders during vacuuming and melting. The pelleted samples were placed in the arc melting system, and the system was first vacuumed up to 10^{-4} millibars and then filled with high purity spectroscopic argon gas (99.999%). In order to homogenize the alloy, it was homogenized for 17 hours at 900 °C under a high purity (99.999%) argon atmosphere, and sudden cooling was applied in salt-ice water and in air. The samples produced in the form of ingots were cut so that DSC, SEM and X-ray measurements could be made. In order to eliminate the difficult effect during cutting, heat treatment was applied to the samples for 30 minutes and then sudden cooling was applied in salt-ice water. The surfaces of the cut alloys were polished to take surface micrographs in order to determine the grain sizes of the instantly cooled samples. The polishing process was done under water in order not to be exposed to heat during polishing. In order to clarify the grain sizes of the polished samples, the samples were etched for 30 seconds in 5 gr $FeCl_3$ + 100 ml methanol + 20 ml HCl solution. X-ray diffractograms of $Ni_{50}Mn_{39}Sn_{11}$ alloy using CuKα (λ=1.5405 Å) radiation, measurements were taken at a constant scanning rate of 2°/min between 2θ = 20° - 80°.

3. Results and Discussion

In Figure 1. a, b, c, d DSC and electrical conductivity curves were given from a part of the samples cut from Ni50Mn39Sn11 alloy, which were subjected to homogenization at 900 °C for 17 hours and instantly cooled in salty-ice water, without applying heat treatment. Phase transformation temperatures of the alloy can be determined by both methods from these graphs [20]. According to DSC curve has been detected which are Austenite start (As): 114 °C, Austenite final (Af): 167 °C Martensite start (Ms):155 °C and Martensite final (Mf):101 °C respectively. These results were determined by using electrical conductivity measurements as As:107 °C, Af:155 °C, Ms:140 °C and Mf :104 °C, respectively Fig 1.b).

The results obtained by both methods are in good agreement. The small difference between the transformation temperatures is the temperature of the heating rate. DSC measurements were taken at a heating-cooling rate of 10 °C/min and resistance measurements 15 °C/min. It is well known that the heating rate in the shape memory alloys has an effect on the transformation temperatures [21, 22].

OM (optical microscopy) images of the alloy taken at different magnifications and room temperature are given in Figure 1.c. It was observed that the grain sizes of alloys were larger than 100 µm. Grain boundaries are evident in surface micrographs. Moreover, it was observed that the martensite plates were cut sharply at these borders. Some of the grains have martensite plates with different orientations. The data obtained from the measurement result were examined for the XRD graph, the peak points were determined by examining the previous studies and are shown in Figure 1.d. Krenke et al. and Chabri et al. stated in their study that the $Ni_{50}Mn_{39}Sn_{11}$ alloy system is of $L2_1$ superlattice type in the austenite phase, and that the $Ni_{50}Mn_{39}Sn_{11}$ alloy in the martensite phase may have 10M, 14M or $L1_0$ crystal structures depending on the amount of Sn [11, 23, 24].

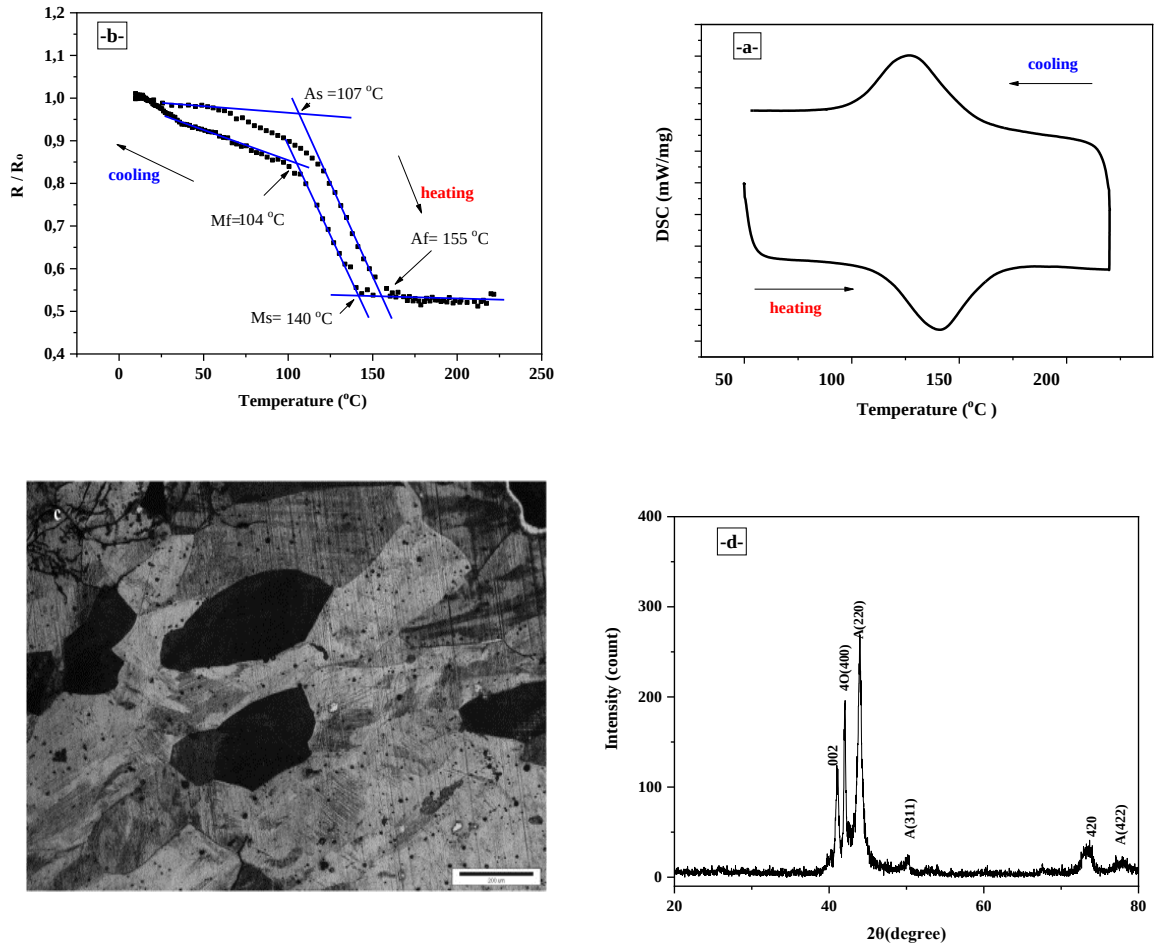

Figure 1. a) DSC curve of non-heat treated $Ni_{50}Mn_{39}Sn_{11}$ alloy **b)** R/Ro changing subject to temperature of non-heat treated $Ni_{50}Mn_{39}Sn_{11}$ alloy **c)** Surface micrographs of $Ni_{50}Mn_{39}Sn_{11}$ alloy **d)** X-ray diffaction pattern of the alloy obtained at room temperature

To investigate the effects of heat treatment on the alloy, two procedures were used. It was heat treated for 60, 120, 180, and 240 minutes at 300 °C. The alloys were then chilled, one at ambient temperature and the other at 0 °C. Figure 2 shows the DSC data obtained following these two heat treatments. As a result of the measurements taken at different scanning speeds, austenite, martensite and enthalpy values were determined. With the increase in the heating rate of the samples cooled in air and water separately at different heating/cooling rates, the austenite start, finish and maximum temperatures also increase, while the martensite start, finish and maximum temperatures decrease in the opposite direction. This is

because the martensite transformation is a phase transformation that occurs at lower temperatures. Depending on the heating rate, the enthalpy values also change. The enthalpy change is related to the amount of conversion of the active phase. If we compare the DSC results of the sample cooled in air and the sample cooled in water, the sample cooled in air transforms at higher temperatures than in water cooling at room temperature. Activation energy was calculated by Kissinger and Ozawa method using DSC measurement results. When activation energies are compared, it is seen that the values found are close to each other.

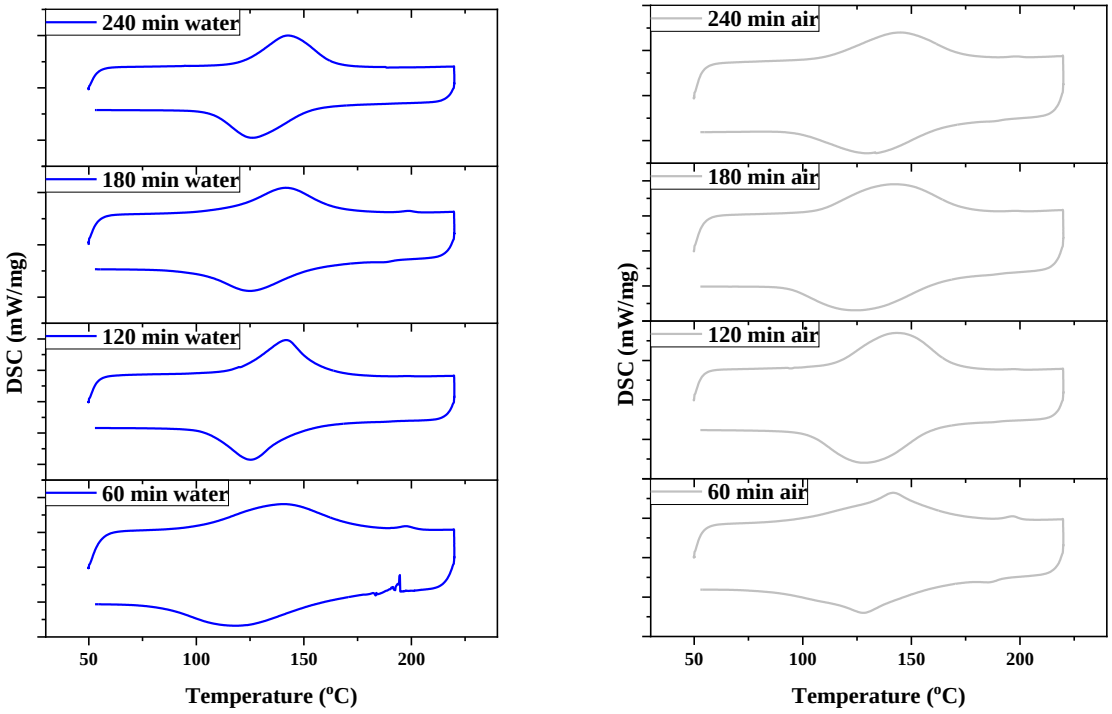

Figure 2. DSC curves of NiMnSn alloy at different conditions **a)** air medium **b)** water medium

DSC experiments were repeated with heating rates of 10 °C, 15 °C, 20 °C, and 25 °C to assess the influence of cooling on activation energy in different mediums after heat treatment. Thermal activation energies were calculated using the Kissinger and Ozawa methods based on the findings of these measurements. Figures 3 and 6 show the linear changes produced using these two methods. Table 1 summarizes the results collected. Table 1 summarizes the average activation energies discovered by both approaches. The untreated alloy has an activation energy of 206.2 J/mol on average. When the activation energies are compared, the values of the activation energies found by the two different methods have values close to each other. This shows that the experimental results are in perfect agreement with each other. But heat treatment time and cooling medium affected the activation energies. This change is given in Figure 7 where it can be seen that the activation energy decreases as the heat treatment time increases in air cooling. On the contrary, the activation energy increased as the heat treatment time increased in the samples cooled in water. At the same time, the activation energy of the sample, which has never been heat treated, was obtained greater than all of them.

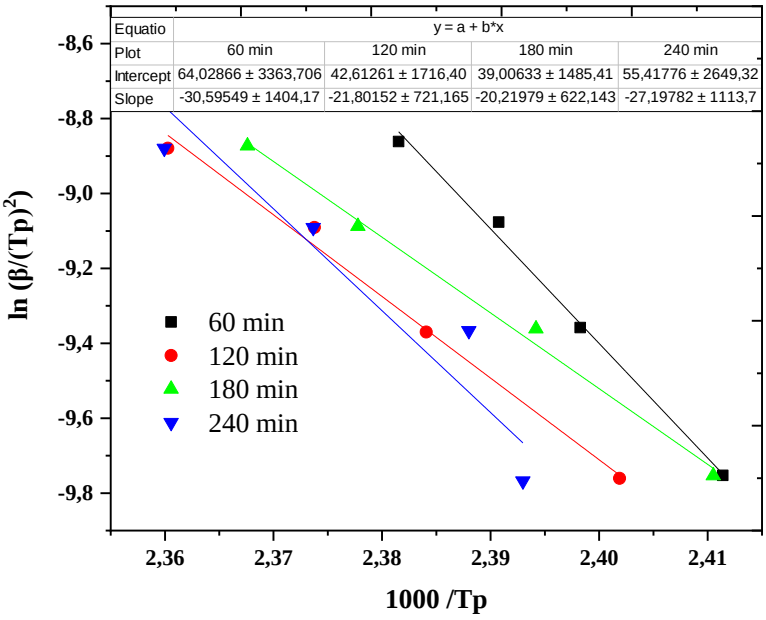

Figure 3. Kissenger plots of alloys cooled in air by heat treatment at 300 °C for 60, 120, 180 and 240 minutes

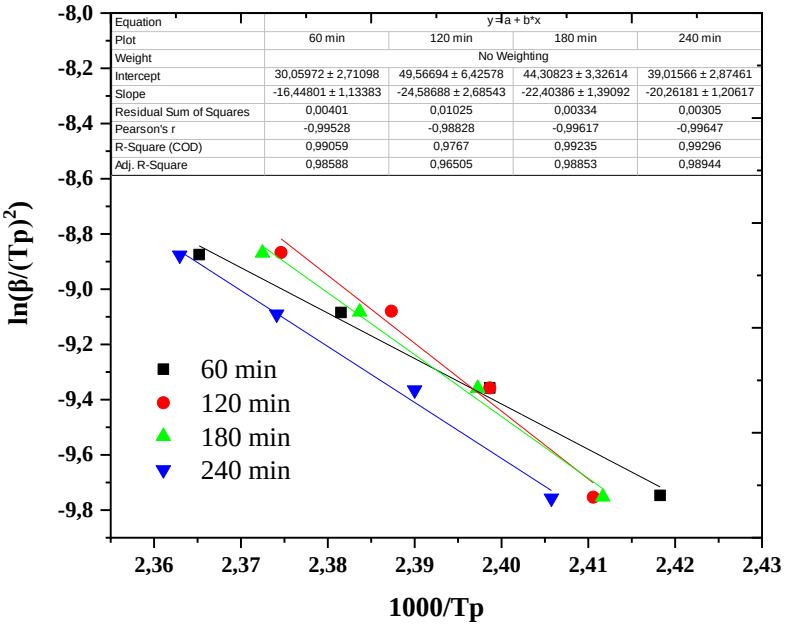

Figure 4. Kissinger plots of alloys cooled in water by heat treatment at 300 °C for 60, 120, 180 and 240 minutes

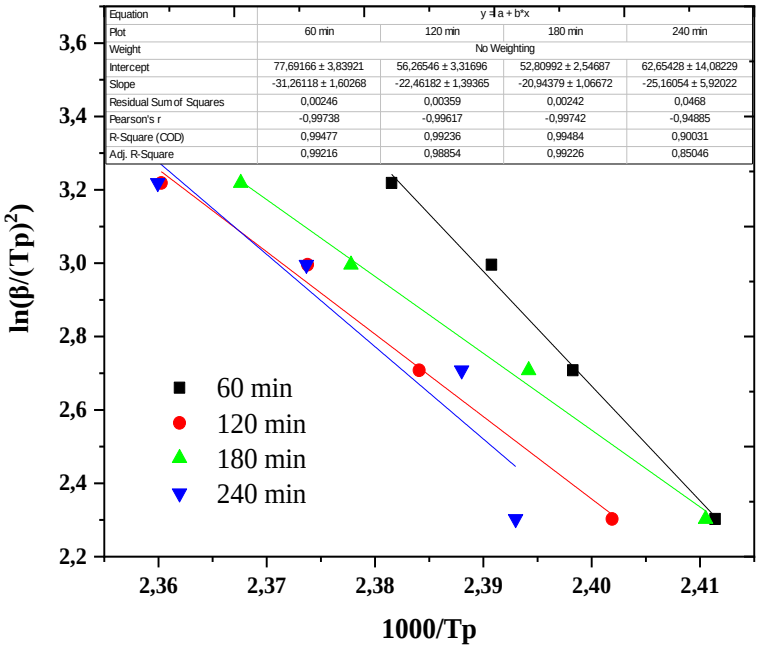

Figure 5. Ozawa plots of alloys cooled in air by heat treatment at 300 °C for 60, 120, 180 and 240 minutes

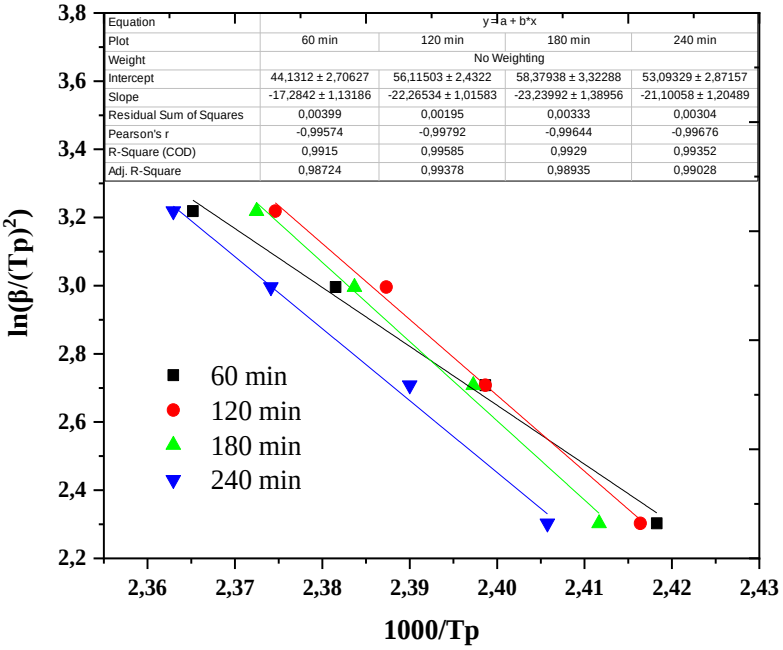

Figune 6. Ozawa plots of alloys cooled in water by heat treatment at 300 °C for 60, 120, 180 and 240 minutes

Table 1. Activation energy values of martensite-austenite transition calculated from Kissinger and Ozawa curves of $Ni_{50}Mn_{39}Sn_{11}$ alloy with different heat treatment and different cooling applied

Methods	Without heat treatment	Heat Treated							
		Air cooling				Water cooling			
Time (min)		60	120	180	240	60	120	180	240
Kissinger M. (J/mol)	208.0	253.0	179.8	167.2	202.2	136.8	204.4	186.3	168.5
Ozawa M. (J/mol)	204.4	247.1	177.5	165.5	198.8	136.6	176.0	183.7	166.8
Ea_{aver} (J/mol)	206.2	250.1	178.7	166.4	200.5	136.7	190.2	185.0	167.7

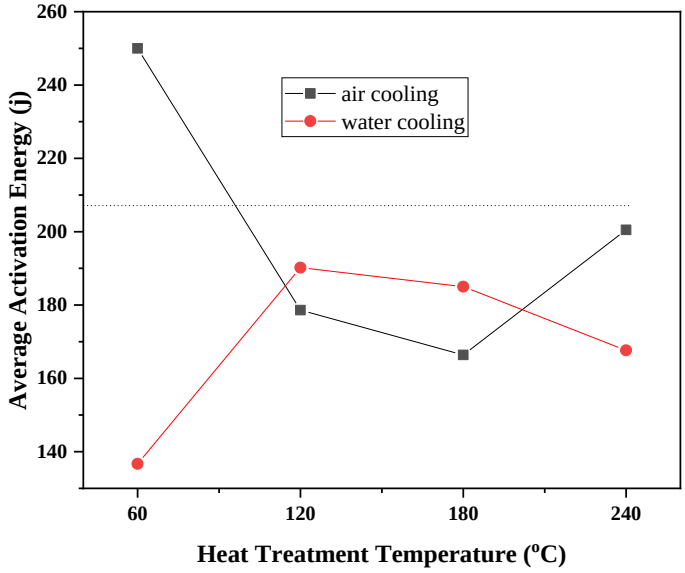

Figure 7. Average activation energy graph of heat treated NiMnSn alloy

Thermal activation energies values of Ni50Mn39Sn11 alloy, which is applied different heat treatment and different cooling, are calculated and given in Table 1. When the activation energies are compared, the values of the activation energies found by two different methods have values close to each other. This shows that the experimental results are in perfect agreement with each other. In order to observe the resistance changes of the $Ni_{50}Mn_{39}Sn_{11}$ alloy with temperature, measurements were taken from room temperature to the temperature range of 0-250 °C, first heating followed by cooling. During the measurement, high purity argon gas was applied at a flow rate of 200 mL/min. to prevent oxidation of the samples in the system. The electrical measurement results obtained are given in Figure 3., Figure 4., Figure 5. and Figure 6. The electrical resistivity of shape memory alloys is sensitive to temperature changes, and electrical resistance-temperature curves can be used to determine transformation temperatures [20]. If the temperature range where the measurements will be taken can be determined correctly, As, Af, Ms, Mf values can be found on these curves. In the resistance-temperature graphs obtained, As, Af, Ms and

Mf temperatures determined in the heating and cooling cycle are in harmony with the transformation temperatures determined by DSC measurements. According to the electrical resistance result of the NiMnSn alloy, it can be said that the resistance of the alloy decreases in the high temperature phase, but increases in the low temperature phase. This result is due to the crystal structure of the alloy in the austenite and martensite phases.

4. Conclusions

In this study, in which the thermal structural and electrical properties of NiMnSn shape memory alloy were investigated, the following results were obtained.

- Phase transition temperatures vary depending on the heating rate. When the DSC graph is examined, it is seen that the probability of austenite peaks returning to martensite peaks is low.
- Activation energies were obtained in accordance with both methods.
- It was found that as the heat treatment temperature increased, the grain size of the alloy decreased.
- It was determined that the transformation temperatures of the alloy could be estimated from the electrical resistance measurements. It was also observed that the alloy exhibited low resistance in the high temperature phase.

Acknowledgements

This work was supported by the Management Unit of the Scientific Research Projects of Gazi University (Project Numbers: 05/2018-04). This article is a part of Master thesis study of Sevim DAĞ.

References

1. Otsuka, K. and X. Ren, Physical metallurgy of Ti–Ni-based shape memory alloys. Progress in materials science, 2005. 50(5): p. 511-678.
2. Otsuka, K. and T. Kakeshita, Science and technology of shape-memory alloys: new developments. mrs bulletin, 2002. 27(2): p. 91-100.
3. Lagoudas, D.C., Shape memory alloys: modeling and engineering applications. 2008: Springer.
4. Srinivasan, A. and D. McFarland, Shape Memory Alloys. PRESS, CU, 2001.
5. Fernandes, D.J., et al., Understanding the shape-memory alloys used in orthodontics. International Scholarly Research Notices, 2011. 2011.
6. Duerig, T.W., K. Melton, and D. Stöckel, Engineering aspects of shape memory alloys. 2013: Butterworth-heinemann.
7. Van Humbeeck, J., Shape memory alloys: a material and a technology. Advanced engineering materials, 2001. 3(11): p. 837-850.
8. Otsuka, K., et al., Mechanism of the shape memory effect in martensitic alloys: an assessment. Philosophical Magazine, 2011. 91(36): p. 4514-4535.
9. Gori, F., et al., A new hysteretic behavior in the electrical resistivity of flexinol shape memory alloys versus temperature. International Journal of Thermophysics, 2006. 27(3): p. 866-879.
10. Acet, M., L. Mañosa, and A. Planes, Magnetic-field-induced effects in martensitic Heusler-based magnetic shape memory alloys, in Handbook of magnetic materials. 2011, Elsevier. p. 231-289.

11. Krenke, T., et al., Martensitic transitions and the nature of ferromagnetism in the austenitic and martensitic states of Ni− Mn− Sn alloys. Physical Review B, 2005. 72(1): p. 014412.

12. Sutou, Y., et al., Magnetic and martensitic transformations of NiMnX (X= In, Sn, Sb) ferromagnetic shape memory alloys. Applied Physics Letters, 2004. 85(19): p. 4358-4360.

13. Kök, M., et al., Effects of Aging on Magnetic and Thermal Characteristics of NiMnCoSn Magnetic Shape Memory Alloys. Iranian Journal of Science and Technology, Transactions A: Science, 2021. 45(6): p. 2191-2199.

14. Qader, I.N., et al., The influence of time-dependent aging process on the thermodynamic parameters and microstructures of quaternary Cu79–Al12–Ni4–Nb5 (wt%) shape memory alloy. Iranian Journal of Science and Technology, Transactions A: Science, 2020. 44(3): p. 903-910.

15. Khalil-Allafi, J., A. Dlouhy, and G. Eggeler, Ni4Ti3-precipitation during aging of NiTi shape memory alloys and its influence on martensitic phase transformations. Acta materialia, 2002. 50(17): p. 4255-4274.

16. Sánchez Llamazares, J.L., et al., Structural and magnetic characterization of the intermartensitic phase transition in NiMnSn Heusler alloy ribbons. Journal of Applied Physics, 2013. 113(17): p. 17A948.

17. Bachaga, T., et al., NiMn-based Heusler magnetic shape memory alloys: A review. The International Journal of Advanced Manufacturing Technology, 2019. 103(5): p. 2761-2772.

18. Kiefer, B. and D.C. Lagoudas, Magnetic field-induced martensitic variant reorientation in magnetic shape memory alloys. Philosophical Magazine, 2005. 85(33-35): p. 4289-4329.

19. Dağ, S., Ni-Mn-Sn şekil hafızalı alaşımların termal ve elektriksel özelliklerinin incelenmesi. 2019, Fen Bilimleri Enstitüsü.

20. Dagdelen, F., et al., Change of electrical resistivity during phase transitions in NiMnSn-based shape memory alloy. Journal of Thermal Analysis and Calorimetry, 2022. 147(10): p. 5815-5823.

21. Balci, E. and F. Dagdelen, The comparison of TiNiNbTa and TiNiNbV SMAs in terms of corrosion behaviour, microhardness, thermal and structural properties. Journal of Thermal Analysis and Calorimetry, 2022. 147(20): p. 10943-10949.

22. Balci, E., et al., Corrosion behaviour and thermal cycle stability of TiNiTa shape memory alloy. Journal of Thermal Analysis and Calorimetry, 2022. 147(24): p. 14953-14960.

23. Chabri, T., A. Venimadhav, and T. Nath, Interplay of austenite and martensite phase inside martensite transition regime and its role on magnetocaloric effect and magnetoresistance in Ni-Mn-Sn based Heusler alloy. Intermetallics, 2018. 102: p. 65-71.

24. Zheng, H., et al., Composition-dependent crystal structure and martensitic transformation in Heusler Ni–Mn–Sn alloys. Acta Materialia, 2013. 61(12): p. 4648-4656.